The International Journal of Advanced Manufacturing Technology (2018) 98:699–713
https://doi.org/10.1007/s00170-018-2306-1

ORIGINAL ARTICLE

Chatter detection and stability region acquisition in thin-walled workpiece milling based on CMWT

Jian Gao [1] · Qinghua Song [1,2] · Zhanqiang Liu [1,2]

Received: 6 February 2018 / Accepted: 5 June 2018 / Published online: 14 June 2018

Abstract

Milling chatter is one of the biggest obstacles to achieve high performance machining operations of thin-walled workpiece in industry field. In the milling process, the time-varying and position-dependent characteristics of thin-walled components are evident. So, effective identification of modal parameters and chatter monitoring are crucial. Although the advantage of chatter monitoring by sound signals is obvious, the milling sound signals are nonstationary signals which contain more stability information both in time domain and frequency domain, and the common analytical transformation methods are no longer applicable. In this paper, short time Fourier transform (STFT) is taken as an example to compare the processing results with cmor continuous wavelet transform (CMWT). This article concerns the chatter detection and stability region acquisition in thin-walled workpiece milling based on CMWT. CMWT combines the advantages of the cmor wavelet and continuous wavelet transform which has good locality and the optimal time-frequency resolution. Therefore, CMWT can be adaptively adjusted signal by the window, which is very suitable for processing nonstationary milling signals. Firstly, the model and characteristics of thin-walled workpiece during the cutting process are presented. Secondly, the CMWT method for chatter detection based on acoustic signals in thin-walled component milling process is presented. And the chatter detection results and stability region acquisitions are analyzed and discussed through a specific thin-walled part milling process. Finally, the accuracy of the method presented is verified through the traditional stability lobe diagram predicted using the exiting numerical method and the machined surface morphologies at different cutting positions obtained through the confocal laser microscope.

Keywords Chatter detection · Thin-walled components · Cmor continuous wavelet transform · Acoustic signal

1 Introduction

Thin-walled workpiece applications in the aerospace industry and the military are becoming increasingly widespread, so efficient milling of thin-walled components is of great significance. However, due to the poor rigidity of thin-walled workpiece, forced vibration and regenerative chatter are easy to occur in the process, which seriously affect the machining efficiency and machining accuracy of thin-walled parts [1] and even the tool life [2]. Therefore, it is important to avoid the occurrence of chatter through effective chatter monitoring measures.

Chatter detection has become the focus of many scholars, and a large number of researches have been carried out. In order to detect the cutting stability, various sensors have been applied, such as displacement sensors [3, 4], accelerometers [5–8], dynamometers [9–13], microphones [14–19], ammeter for motor current [20, 21], and multisensors [22]. Both the appropriate sensors and the matching signal processing methods are essential for the monitoring of chatter [23]. However, during the milling process, the thin-walled component has obvious deformation and the modal characteristics change with the material removal process (the time-varying

✉ Qinghua Song
ssinghua@sdu.edu.cn

Jian Gao
gaojian_n@126.com

Zhanqiang Liu
melius@sdu.edu.cn

[1] Key Laboratory of High Efficiency and Clean Mechanical Manufacture, Ministry of Education, School of Mechanical Engineering, Shandong University, Jinan, People's Republic of China

[2] National Demonstration Center for Experimental Mechanical Engineering Education, Shandong University, Jinan, People's Republic of China

characteristic). Meanwhile, the modal parameters also vary with the milling position (position-dependent characteristic). Therefore, both time-varying characteristic and position-dependent characteristic of thin-walled workpiece milling should be considered during the chatter monitoring [1, 24]. For nonstationary systems, the acoustic signal can contain more information both in time domain and frequency domain, and acoustic signals are also easily collected by the microphone, so the milling acoustic signal is the best choice for chatter detection.

Common methods of chatter monitoring include fast Fourier transform (FFT), short time Fourier transform (STFT), Gabor transform (GT), wavelet transform (WT) [12, 23], wavelet packet decomposition (WPD) [25], wavelet modulus maxima (WMM) [26], Wigner distribution (WD), and so on. FFT can convert the signal from time domain to frequency domain. However, FFT only has the characteristics of frequency analysis, cannot show how the transient frequency of the signal changes over time [27]. The Gabor transform is affected by the size of the window, so its analysis is less precise and easier to be affected by various noise. Due to the limitation of window function, FFT, STFT, and GT cannot perform multi-scale analysis on the milling acoustic signal. Therefore, the influence of the time-varying and position-dependent characteristics of the thin-walled components milling on the chatter monitoring is neglected, which leads to the chatter detection results that are not accurate. However, the wavelet methods mentioned above are able to decompose the signal by variable scale time-frequency factor, so that multi-scale and variable frequency analysis of different frequency bands of signals can be implemented [28].

Most wavelet monitoring methods are used in chatter monitoring. Tangjitsitcharoen et al. [12, 23] proposed to use wavelet transform to monitor the ball head milling process. Before the wavelet transform, the dynamic milling force is decomposed into four levels according to a certain ratio. Then, a different algorithm is used to detect the chatter. Yao et al. [29] proposed an online identification method for early chatter. By combining the advantages of wavelet transform and support vector machine, the accuracy of chatter monitoring is effectively improved. Cao et al. [30] proposed a chatter recognition method based on wavelet transform and Hilbert-Huang transform. Using the Hilbert-Huang spectrum as chatter indices, the signals are analyzed using WPD and HHT. However, the efficiency of obtaining Hilbert-Huang spectrum is quite low, which limits the effectiveness of online monitoring. Jiang et al. [31] exploited the WPD method to deal with the signal and then use the Hidden Markov Model and support vector machine to predict the chatter on signal that has been decomposed. Chen et al. [32] proposed a method of online monitoring chatter based on wavelet packet transform (WPT) and support vector machine recursive feature elimination (SVM-RFE). By applying this method to incipient chatter, it is shown that the impulse factor and one-step autocorrelation function were the sensitive chatter features. Zhang et al. [33] used wavelet packet decomposition to decompose the cutting force signal into multiple sub-signals and monitoring chatter based on the energy entropy which was extracted from sub-signals. Sun et al. [34] proposed a method of online monitoring chatter based on weighted wavelet entropy to detect the chatter of the turning process. Wang et al. [35] presented a method for monitoring chatter based on discrete wavelet transform (DWT) and wavelet modulus maxima (WMM). However, there are always some shortcomings for the wavelet method mentioned above. For example, in the WPD method, the number of decomposed layers directly affects the chatter monitoring results, so the selection of decomposition level is particularly important, but at present, the number of decomposed layers is selected based on experience, which leads to the tedious monitoring process and inaccurate results of chatter detection. In addition, the selection of the wavelet basis function and the threshold size affect the chatter monitoring effect, and the threshold is not easy to be determined. When the threshold is too large, it is easy to ignore some chatter signals. When the threshold is too small conversely, it is easy to cause misjudgement. Therefore, the existing wavelet methods have some key shortcomings for nonstationary milling signals. These wavelet methods do not apply to the chatter detection of thin wall workpiece milling.

The cmor continuous wavelet transform (CMWT) used in this paper not only does not involve the number of decomposition layers and the threshold size, but cmor wavelet can be selected adaptively. Since cmor wavelet has a unique advantage in the field of nonstationary signal analysis, CMWT can be applied to a variety of acoustic signals including milling acoustic signal. After absorbing the advantages of cmor wavelet, CMWT is a time-frequency analysis method which can be adaptively adjusted by window. Besides, CMWT has simple operation, and the efficiency of chatter detection is obvious. Thus, the focus of the paper is the chatter detection of thin-walled workpiece milling. The acoustic signals collected in the milling experiment are processed by CMWT to obtain 2D and 3D time-frequency diagram. Whether the chatter occurs during the milling process can be easily judged from time-frequency diagram. And stability lobe diagram predicted and surface topography observation are employed to confirm the accuracy of the method for chatter monitoring. The remainder of this paper is summarized as follows. Analysis of milling characteristics of thin-walled component and identification of modal parameters are presented in Section 2. The CMWT method in milling process is proposed in Section 3. The results of chatter detection and verification are shown in Section 4. The conclusions are drawn in the last section.

2 The milling model of thin-walled workpiece

2.1 The milling characteristics

In the milling system of thin-walled workpiece, the thin-walled components are flexible parts, which can be significantly deformed under the cutting force due to their weak rigidity. Chatter may occur in the deformation process of thin-walled workpiece, which is accompanied by a large number of noise, resulting in obvious vibration marks on the machined surface.

The milling characteristics of thin-walled components include the time-varying characteristics besides the easy deformed characteristics mentioned above [36]. Time-varying characteristics also include two aspects. On the one hand, the process of the material removal (Δm_i) will change the modal characteristics of the thin-walled parts, as shown in Fig. 1a, such as the natural frequency and rigidity of the thin-walled workpiece change with the removal of the material. On the other hand, the modal parameters of the thin-walled parts vary with the milling position. In other words, the modal parameters of the thin-walled parts are related to its modal shapes as shown in Fig. 1b.

According to the milling characteristics of the thin-walled parts, the cantilever thin-walled rectangular plate is used as a simplified model of thin-walled workpiece, with the length L, width W, and thickness H, as shown in Fig. 1a. In order to describe the time-varying characteristics, the thin-walled plate model is discreted into a finite element model, consisting of many discrete points, as shown in Fig. 2. During the milling process, the response of the contact area between the tool and the thin-walled plate directly reflects the time-varying characteristics. It is assumed that the s-order mode dominates the vibration. When the tool moves to the point u along the cutting path, the governing equation of the point u is

$$\frac{m_s}{\varphi_{us}^2}\ddot{x}_u + \frac{c_s}{\varphi_{us}^2}\ddot{x}_u + \frac{k_s}{\varphi_{us}^2}\ddot{x}_u = F_t \tag{1}$$

where m_s is modal mass, c_s is modal damping, k_s is modal stiffness, φ_{us} is the u-term of the eigenvector of the s-order modal, and F_t is the cutting force. Similarly, when the tool moves to point v, the v- term of the s-order modal eigenvector is expressed by φ_{vs}. Obviously, $\varphi_{us} \neq \varphi_{vs}$. Therefore, the modal parameters have the characteristic of the positional dependence. The modal parameters at the point u are defined as m_{us}, c_{us}, and k_{us}, and the modal parameters at the point v are defined as m_{vs}, c_{vs}, and k_{vs}.

From Eq. (1), the following expression can be obtained

$$\frac{m_{us}}{m_{vs}} = \frac{c_{us}}{c_{vs}} = \frac{k_{us}}{k_{vs}} = \frac{\varphi_{vs}^2}{\varphi_{us}^2} \tag{2}$$

Therefore, it can be concluded that the modal parameters of thin-walled workpiece are related to the modal shapes of their corresponding points, and the ratio of modal parameters is inverse to the modal square of the corresponding points [26]. Considering the modal and time-varying characteristics of thin-walled component, it is necessary to find an effective way to analyze the transient response during milling, which is very important for chatter detection.

2.2 Modal parameter identification

Both the chatter detection and verification require the modal parameters and the loss factor of the system. The damping ratio of the workpiece-fixture system is usually less than 0.05, so the damping ratio ξ of the system can be obtained by using the half-power bandwidth method, and then the loss factor η of the system also can be expressed as

$$\eta = 2\xi \tag{3}$$

Assuming that the thin-walled system resonates at the s-order modal, i.e., $\omega = \omega_s$. Since the modal density of the resonance region is relatively small, the influence of other modes can be ignored. Therefore, when the point u is excited, the FRF expression at point-l is as follows [37]

$$H_{lu}(\omega) = \frac{A_{lus}}{\alpha\omega_s - \omega} + \frac{-A_{lus}}{-\alpha\omega_s - \omega} \tag{4}$$

where,

$$\alpha = \sqrt{1 + j\eta}, \quad A_{lus} = \frac{\varphi_{us}\varphi_{ls}}{2\alpha\omega_s m_{us}} \tag{5}$$

For the convenience of calculation, it is assumed that the modal shape at the machining location is 1; hence, the modal mass, modal stiffness, modal damping at the machining position are as follows

$$m_{us} = \frac{1}{|2A_{uus}\alpha|}, \quad k_{us} = m_{us}\omega_s^2, \quad c_{us} = 2m_{us}\xi_s\omega_s \tag{6}$$

3 Cmor continuous wavelet transform in milling process

3.1 Typical nonstationary signal in milling process

The acoustic signal in the milling process is a typical nonstationary signal, and its autocorrelation function and power spectral density are generally time-varying [38]. For such a signal, it is not enough to know the single global characteristic of the signal in the time domain or frequency domain only by traditional method, such as Fourier transform, and it is also

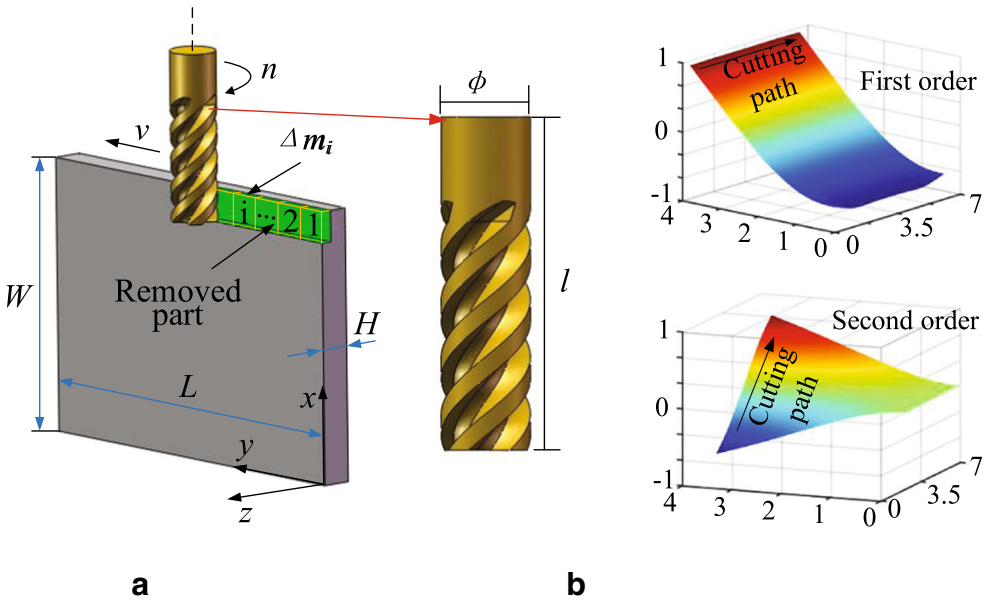

Fig. 1 The milling dynamic model of thin-walled workpiece. **a** Material removal process. **b** First two mode shape

necessary to understand the change of the spectrum of the signal with time.

In order to make up for the deficiency of Fourier transform and realize the local analysis of nonstationary signals, continuous wavelet transform (CWT) can be used to establish a joint function about time and frequency that maps 1D time signal to a 2D time scale (time-frequency) and describes the energy density and intensity of the signal at different times and frequencies. CWT uses variable scale time-frequency factors to decompose signals, so as to realize multi-scale analysis and frequency analysis for different frequency bands of signals. CWT not only can accurately locate the corresponding frequency components at a certain moment but also can accurately locate the corresponding time of a certain frequency component.

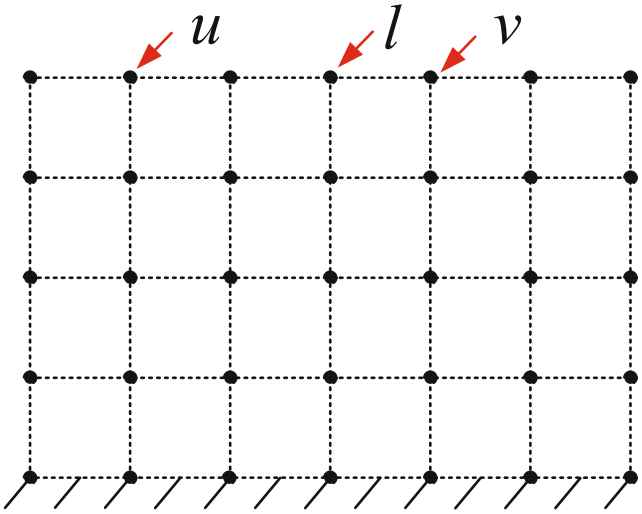

Fig. 2 The discrete plate model

3.2 CWT for milling process

In view of time-varying characteristics of autocorrelation function and power spectral density of nonstationary signal, CWT uses variable scale time-frequency factors to analysis signals, so as to realize multi-scale analysis and frequency analysis for different frequency bands of signals.

The basic calculation method of CWT is numerical integration approximation, which includes rectangular numerical integration method and trapezoidal numerical integration method. In order to make the calculation result more accurate, the latter method is used to do approximate integral as follows

$$\begin{aligned} WT_f(a,b) &= \frac{1}{\sqrt{a}}\int_{-\infty}^{+\infty} f(t)\psi^*\left(\frac{t-b}{a}\right)dt = \langle f(t), \psi_{a,b}(t)\rangle \\ &= \int_{-\infty}^{+\infty}\frac{1}{C_\psi}\left(\int_0^{+\infty}\int_{-\infty}^{+\infty} WT_f(a,b)\psi_{a,b}\frac{1}{a^2}dadb\right)\psi^*(t)dt \end{aligned} \tag{7}$$

where b is the translation factor, $b = kT_s$, $t = nT_s$; T_s is sampling interval, a is a scale, usually $a = 1/2^j$, and j is the resolution; $f(t)$ stand for signals with limited energy; and $\psi^*(t)$ represents the complex conjugate of wavelet $\psi(t)$.

When the base wavelet satisfies the admissible condition, its inverse transformation is

$$f(t) = \iint W_f(a,b)\psi_{a,b}(t)dbda \tag{8}$$

The scale a is not directly related to the frequency f, but the smaller the a, the smaller the wavelet period, the higher the corresponding frequency; the larger the a, the larger the wavelet period, the lower the corresponding frequency.

When the wavelet function and sampling period have been determined, the scale and frequency need to be corresponded. Next, it is necessary to find a virtual frequency corresponding

to the certain scale, so the scale a corresponding virtual frequency f_a can be calculated as follows

$$f_a = \frac{f_c}{a \times \Delta} \tag{9}$$

where Δ is the sampling period and f_c is wavelet center frequency.

Although CWT is very suitable for processing the acoustic signals in milling, it is still necessary to choose the wavelet function carefully in order to get the optimal time-frequency resolution. The selection of wavelet function can directly influence the local analysis characteristics of CWT in the time and frequency domain of the milling signal. Besides, thin-walled component milling system has time-varying characteristic and position-dependent characteristic, and these characteristics are also hidden in the milling acoustic signal, so it is necessary to choose a wavelet function that can handle the time-varying and position-dependent characteristics of the acoustic signal in time and frequency domain flexibly. Therefore, the cmor wavelet is adopted in this paper.

3.3 Cmor CWT for milling process

The cmor wavelet is adopted in CWT here, which named CMWT. The cmor wavelet is the complex form of Morlet wavelet. The Morlet wavelet consists of a sinusoidal wave modified by a Gaussian envelope, so it is given as [28]

$$\psi(t) = C \cdot e^{-t^2/2\sigma^2} e^{i\eta t} \tag{10}$$

where η is the center frequency, σ the shape parameter, and C is a constant which should be chosen on different occasions.

From Eq. (10), the two obvious advantages of Morlet wavelet can be found. On one hand, the Morlet wavelet has the optimal time-frequency resolution for nonstationary milling signal. Reference [39] pointed out: the parameter σ balances the time resolution and the frequency resolution of the Morlet wavelet. An increase in σ will increase the frequency domain resolution. A reduction in σ will increase the resolution in the time domain. When $\sigma \to \infty$, the Morlet wavelet becomes a cosine function which has the finest frequency resolution, and when $\sigma \to 0$, the Morlet wavelet becomes a Dirac function which has the finest time resolution. Besides, the literature [40] verifies the above conclusions by means of quantitative calculation based on Heisenberg triangle. Because of the time-varying nature of the thin-walled workpiece milling process, time-frequency analysis of milling signals is crucial. Therefore, if the appropriate σ is determined, CMWT will have the optimal resolution both in time domain and frequency domain in the processing of milling signals.

On the other hand, the Morlet wavelet has good locality in both time domain and frequency domain. The expression of Morlet wavelet in time domain and frequency domain is as follows

$$\varphi(t) = e^{-t^2} e^{j\omega t}, \quad \phi(\omega) = \sqrt{2\pi} e^{-(\omega-\omega_0)^2/2} \tag{11}$$

It can be viewed on Eq. (11) that ω only affects the imaginary part, and the envelope region of $\varphi(t)$ does not change with the change of ω; ω_0 is the center frequency of $\varphi(\omega)$, and the bandwidth of $\varphi(\omega)$ remains the same with ω_0 changes [26]. Therefore, the Morlet wavelet has good locality in both time domain and frequency domain. Based on the above feature, CMWT can handled milling signal that both the autocorrelation function and the power spectral density change with time by adaptively adjusted window.

In addition to the above two advantages, the cmor wavelet also has a larger bandwidth and center frequency, and the time-frequency diagram after wavelet transform shows better time-frequency aggregation.

CMWT combines the advantages of the cmor wavelet and CWT, which are very suitable for processing nonstationary signals. CMWT is a time-frequency analysis method which can be adaptively adjusted by the window. When detecting high frequency information, the time window is automatically narrowed, and when detecting low frequency signals, the time window is automatically widened. CMWT has high time resolution and low frequency resolution at high frequency and has higher frequency resolution and lower time resolution at low frequency. Therefore, CMWT has obvious benefits in the analysis and processing of nonstationary signals in milling process.

4 Results and discussions

4.1 Experiment setup

The workpiece is a rectangular thin-walled aluminum alloy plate (7075T); in addition, the geometric parameters are shown in Table 1. The four-tooth end mill is used in milling experiment. Its diameter d is 12 mm, the overhang length l is 43 mm, the helix angle is 45°, and the material is cemented carbide, so the tool can be assumed to be rigid. In order to guarantee the universality of the experiment, those experiments are in the conventional boundary conditions: the bottom of the workpiece ($y = 0$) completely ($0 \le y \le 0.07$ m) fixed and the other three edges free.

In order to obtain modal parameters, hammer mode experiment (I) is required. After that, milling experiment (II) was conducted and acoustic signals were collected to monitor the chatter. Both hammer mode experiment and milling

Table 1 Geometrical parameters of workpiece

Material	Cantilever size (mm)			Density (kg/m3)	Young's modulus (GPa)	Poisson's ratio
	Length	Width	Height			
Al 7075	70	40	5	2.81×10^3	71.7	0.33

experiment were performed on a VMC0540d CNC machine with a maximum spindle speed of 30,000 rpm.

The main purpose of hammer mode experiment is to obtain the natural frequency ω_n and the loss factor η of the workpiece-machine tool system, which is a necessary element to detect chatter and draw the stability lobe diagram (SLD). It is worth mentioning that, due to the limitation of the modal parameter extraction method, the hammer and accelerometer must be in the form of "point-to-point" percussion, as shown in Fig. 3b. The rest equipment of hammer mode experiments include a B&K data acquisition box, an accelerometer with a sensitivity of 98.45 mv/g, a hammer, and a matching computer, as shown in Fig. 3b. The schematic diagram of hammer mode experiment is shown in Fig. 3a. The equipment for milling experiment are shown in Fig. 3c.

Before the hammer mode experiment, the modal analysis results of thin-walled plate are the first three natural frequencies are 2873.1, 4461.5, and 8768.0 Hz, respectively. Through the hammer mode experiment, the first-order natural frequency ω_n is 2713 Hz, which is very close to the first-order natural frequency (2873.1 Hz) in computer simulation.

In order to monitor chatter effectively, GRAS40pp micro-microphone was used to collect acoustic signals, with sensitivity of 50 mv/Pa. The surface topography of the machined surface was observed by 3D confocal laser microscope shown in Fig. 3d.

4.2 Result analysis

4.2.1 Selected acoustic signal

In the milling experiment, the up milling and vertical milling are adopted, the feed rate of the tool is 420 mm/min, and the milling time of each workpiece is exactly 10 s. In addition, only the spindle speed and axial milling depth were changed, and the specific cutting parameters are shown in Table 2. During the milling process, the acoustic signal is collected to monitor the chatter.

The selected acoustic signals shown in Fig. 4 are collected from text no. 14 (Fig. 4a), test no. 5 (Fig. 4b), and test no. 8 (Fig. 4c), respectively. Obviously, the above three acoustic signals of experiments are symmetrically distributed which fully conform to the modal characteristics of thin-walled plates.

The shape of the acoustic signal in test no. 14 is similar to dumbbell, and the acoustic pressure is the maximum in two periods of 0~1.7 and 8.3~10 s, about 8 Pa. During two periods of 1.7~2.5 and 7.5~8.3 s, the acoustic pressure decreased and increased, respectively. The average value of acoustic pressure decreased from 8 to 3 Pa of 1.7~2.5 s, and the average value of acoustic pressure in 7.5~8.3 s increased from 3 to 8 Pa. The acoustic pressure is the minimum in 2.5~7.5 s, about 3 Pa. The change trend of the acoustic signal in test no. 5 is similar to this in test no. 14, except that the period of maximum sound pressure is shortened to 0~1 and 9~10 s, and the average of acoustic pressure is about 7 Pa in two periods. The period of minimum sound pressure about 3 Pa is extended to 1.4~8.6 s. In particular, the acoustic signal in test no. 8 is evenly distributed, and the acoustic pressure in the entire period is basically equal and the acoustic pressure is approximately 4 Pa.

4.2.2 Chatter monitoring process using CMWT

In order to judge the steady state of milling through sound signals, several representative signal segments (S_1~S_7) are selected from the three groups of acoustic signals. The CMWT method is used to process the selected acoustic signal to obtain the time-frequency diagram which makes the stable

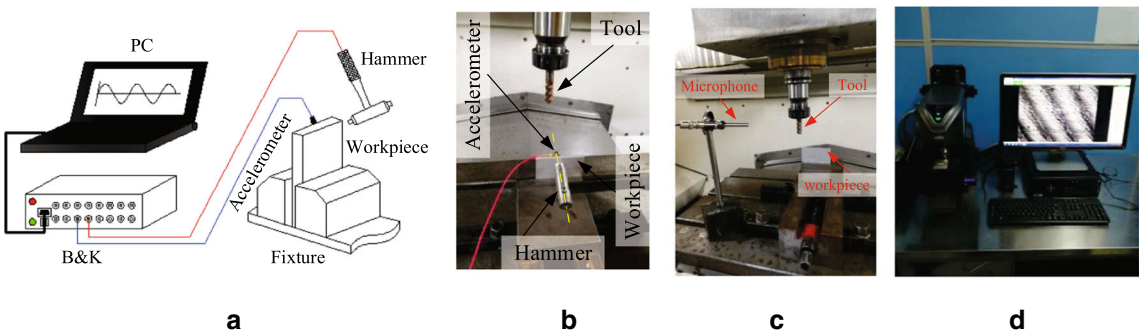

Fig. 3 Experiment setup. **a** The schematic diagram. **b** Experiment I setup. **c** Experiment II setup. **d** 3D microscope

Table 2 The specific cutting parameters

Group	Test	Spindle speed (rpm)	Radial depth of cut (mm)	Axial depth of cut (mm)	Feed speed (mm/min)
I	No. 1	7000	1	5	420
	No. 2	7000	1	5	420
	No. 3	7000	1	5	420
II	No. 4	8500	0.7	5	420
	No. 5	8500	1.0	5	420
	No. 6	8500	1.3	5	420
	No. 7	8500	1.6	5	420
III	No. 8	11,000	0.5	5	420
	No. 9	11,000	0.9	5	420
	No. 10	11,000	1.3	5	420
	No. 11	11,000	1.7	5	420
IV	No. 12	14,000	1.0	5	420
	No. 13	14,000	1.5	5	420
	No. 14	14,000	2.0	5	420
	No. 15	14,000	2.5	5	420

domain and the chatter frequency bandwidth of the thin-walled plate easily obtained.

Firstly, because the second-order natural frequency of the workpiece is much larger than the first-order natural frequency, the effect of the second-order natural frequency on the chatter can be neglected. Therefore, when monitoring chatter, only the influence of first-order natural frequency is considered. Secondly, the tooth passing frequency appears as a harmonic form in the milling which will have an effect on chatter detection. In addition, an integer multiple of the tooth passing frequency is no exception, which is called frequency multiplication. However, the effect of tooth passing frequency on chatter is far from the natural frequency. The impact of the tooth passing frequency and the natural frequency can be easily distinguished from the time-frequency diagram obtained by the CMWT, which is also the advantage of using CMWT to monitor chatter.

For test no. 14, the selected signal segments are S_1 (0.5~1.3 s), S_2 (4.5~5.3 s), and S_3 (7.5~8.3 s), as show in Fig. 4a. In test no. 14, the tooth passing frequency ω_t is 933 Hz and the frequency multiplications are 1866, 2799, 3732, and 4665 Hz, respectively. The 2D time-frequency diagram (Fig. 5b) of S_1 obtained from CMWT shows that there is a clear and continuous green band near the natural frequency of the workpiece, while the remaining bands in the Fig. 5b are discontinuous, which occurs near the frequency multiplication of the tooth passing frequency. At the same time, the maximum value of the wavelet coefficients in the 3D time-frequency graph appears near the natural frequency ($A_1 > A_2$). Therefore, it can be confirmed that the chatter occurs in S_1 and the chatter frequency band is 2.7~3 kHz.

In contrast, there are only some discontinuous yellow bands in the 2D time-frequency diagram of S_2 (Fig. 5e), which occurs at $2\omega_t$ and $3\omega_t$, and $2\omega_t$ is dominant. Besides, the amplitude of the wavelet coefficients in the 3D time-frequency diagram (Fig. 5f) is relatively small, so that it is easy to judge that the S_2 is in a stable state and no chatter occurs. For S_3, from the 2D time-frequency diagram (Fig. 5h), it can be intuitively found that both continuous and discontinuous bands are gradually appearing, widen and brighten from left to right. The continuous band is near ω_n while discontinuous band is near $3\omega_t$. The amplitude of the wavelet coefficients in the 3D time-frequency diagram (Fig. 5i) also increases from left to right, and the band near the natural frequency is brighter and higher ($A_4 > A_3$). It can be judged that S_3 is in a transition state and the transition from stable state to chatter state.

For test no. 5, the selected signal segments are S_4 (0~0.7 s), S_5 (1~1.4 s), and S_6 (5.6~6.4 s), as shows in Fig. 4b. In test no. 5, tooth passing frequency ω_t is 567 Hz and frequency multiplication are 1134, 1701, 2268, 2835, and 3402 Hz, respectively. The analysis of the acoustic signal of test no. 5 is similar to the analysis of test no. 14 above, so it can be concluded from Fig. 6 that chatter occurs in S_4 and the chatter frequency band is 2.8~3.1 kHz; S_5 is in transition state which from chatter to stable; and S_6 is in stable state.

Similarly, for test no. 8, the selected signal segment is S_7 (0~1.5 s), as shown in Fig. 4c. In test no. 8, tooth passing frequency ω_t is 733 Hz and frequency multiplications are 1466, 2199, 2932, and 3665 Hz, respectively. A conclusion from Fig. 7 can be drawn: S_7 is only affected by the frequency multiplication of tooth passing frequency and the whole milling process is in steady state.

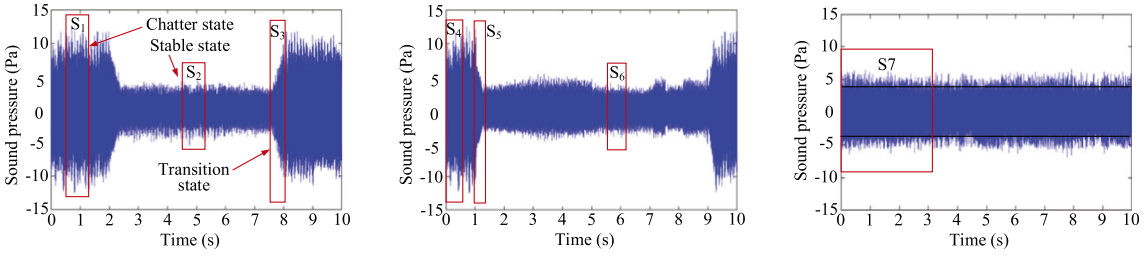

Fig. 4 Recorded acoustic signal in the microphone. **a** Acoustic signal for test no. 14. **b** Acoustic signal for test no. 5. **c** Acoustic signal for test no. 8

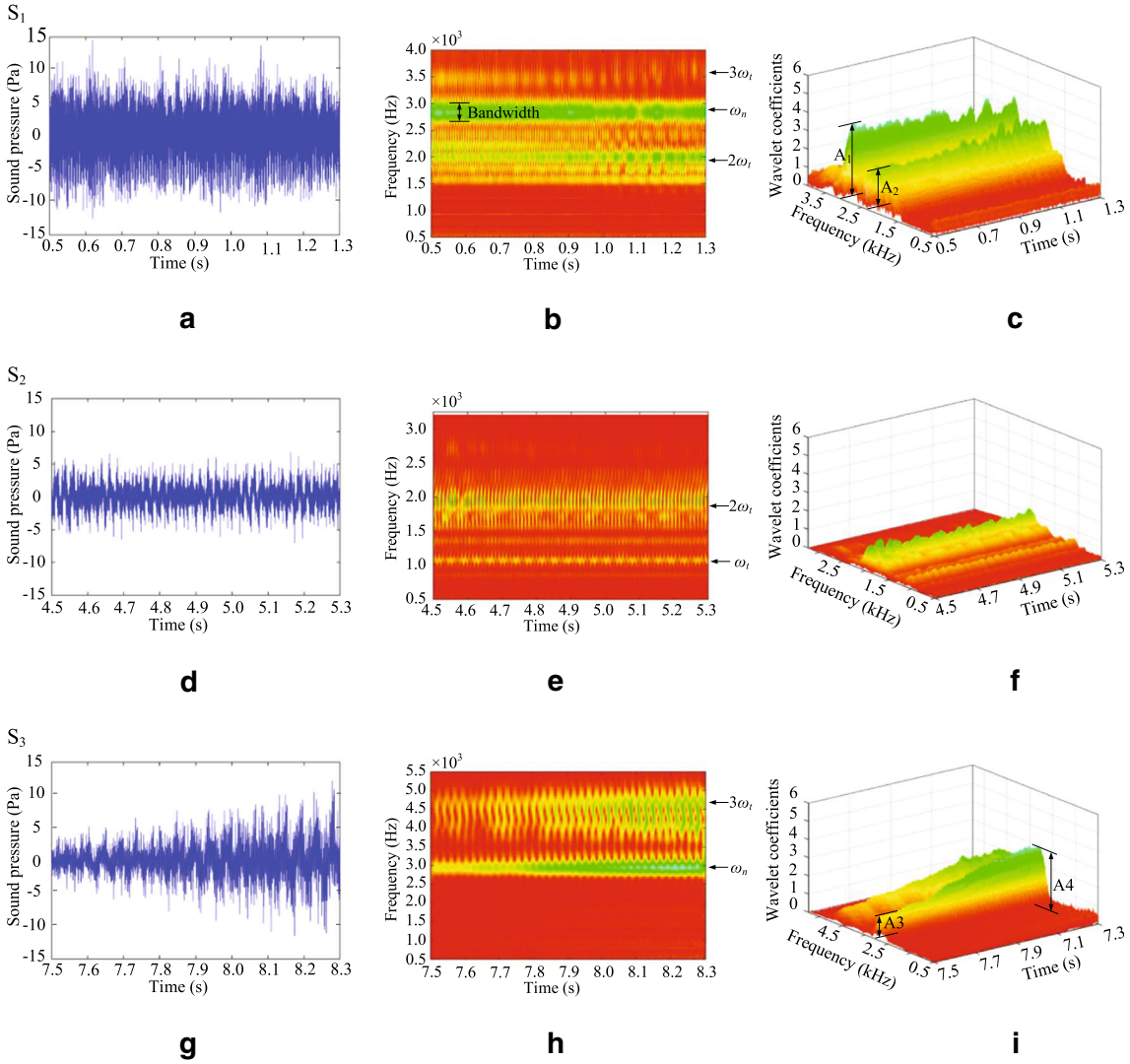

Fig. 5 CMWT of acoustic signals obtained from test no. 14. **a** Time domain diagram. **b** Time-frequency domain diagram. **c** 3D diagram. **d** Time domain diagram. **e** Time-frequency domain diagram. **f** 3D diagram. **g** Time domain diagram. **h** Time-frequency domain diagram. **i** 3D diagram

Although thin-walled parts have time-dependent and position-dependent characteristics, the CMWT is still suitable for chatter monitoring of thin-walled parts and has a remarkable advantage in the process of chatter monitoring for thin-walled parts. There is no redundant frequency band interference in the CMWT processing results, and the numerical error of the frequency band is so small that it can be ignored, and the process of the CMWT processing sound signal is not disturbed by noise. Through the analysis of the 2D and 3D time-frequency diagram obtained by CMWT, once the natural frequency of the thin-walled workpiece and the tooth-through frequency of the milling system are obtained, it is possible to monitor whether or not chatter occurs by 2D and 3D time-frequency diagrams. The stability of thin-walled parts can be obtained intuitively. Meanwhile, CMWT improves the efficiency of chatter monitoring, effectively shortens the time of chatter monitoring, less than 0.2 s, and lays a solid foundation for the following online chatter detection.

4.2.3 Comparison and analysis of STFT method

There are many traditional chatter monitoring methods, including FFT, STFT, WPD, and so on. In the WPD method, the number of decomposed layers directly affects the chatter monitoring results, so the selection of decomposition level is particularly important [41], but at present, the number of decomposed layers is selected based on experience, which leads to the result of chatter detection is accidental. Therefore, in order to avoid the influence of accidental factors, in this paper, STFT is used as a comparison method for chatter monitoring.

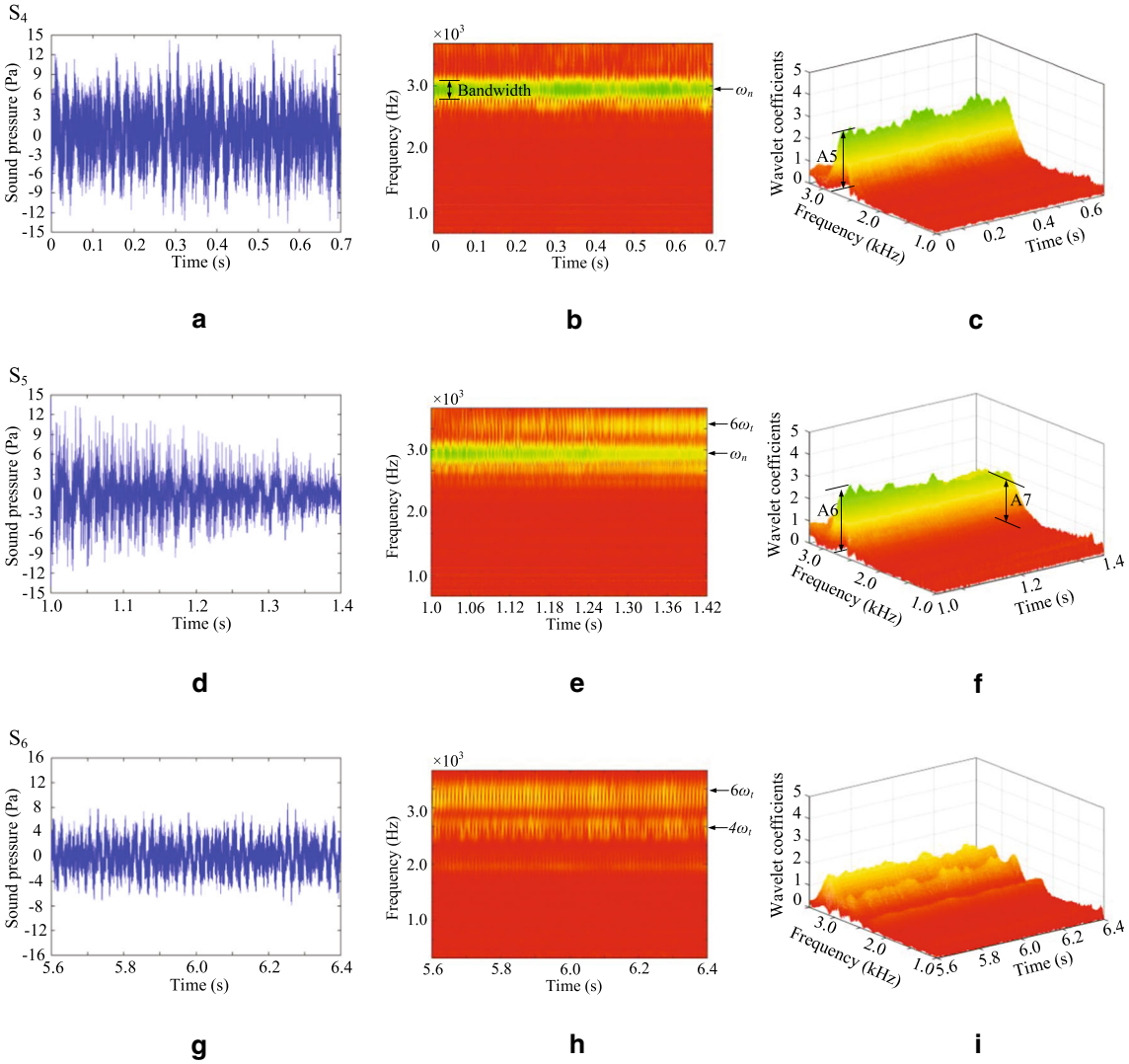

Fig. 6 CMWT of acoustic signals obtained from test no. 5. **a** Time domain diagram. **b** Time-frequency domain diagram. **c** 3D diagram. **d** Time domain diagram. **e** Time-frequency domain diagram. **f** 3D diagram. **g** Time domain diagram. **h** Time-frequency domain diagram. **i** 3D diagram

In STFT, directly adding a rectangular window to the signal will cause a frequency leakage [42]. In order to avoid the frequency leakage, the Hamming window is used in this paper. The amplitude-frequency characteristic of the Hamming window is that the sidelobe attenuation is larger, and the peak value of the main lobe and the first sidelobe can be reduced by 40 db [43].

After CMWT processing and analysis, it can be concluded that S_1 and S_4 are in a chatter state, S_3 and S_5 are in a transition state, and S_7 is in a stable state. Therefore, the time-frequency

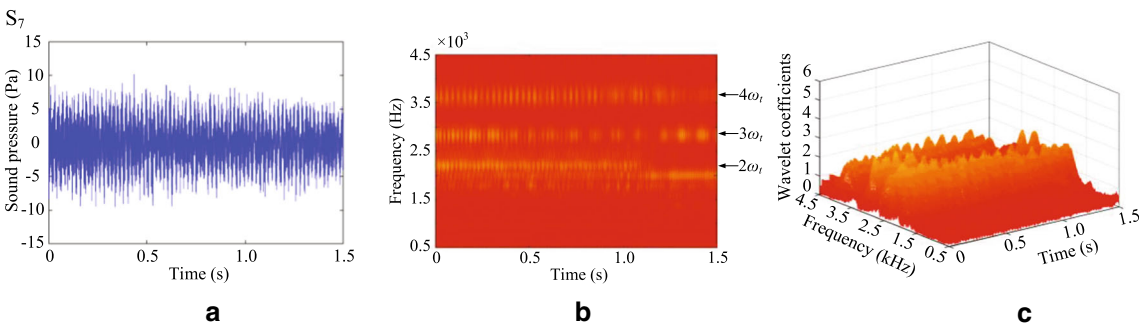

Fig. 7 CMWT of acoustic signals obtained from test no. 8. **a** Time domain diagram. **b** Time-frequency domain diagram . **c** 3D diagram

analysis was performed on the typical acoustic signals of S_1 and S_4, S_3 and S_5, and S_7 using STFT, and the results are shown in Fig. 8.

Through the analysis of Fig. 8, we can draw the following conclusions. Firstly, from the processing results of STFT, there are some deviations between the highlighted red frequency band and its corresponding natural frequency, tooth pass frequency, and tooth pass frequency multiplication and the error is within ± 50 Hz. This is mainly because thin-walled parts have multi-modal coupling characteristics, and milling

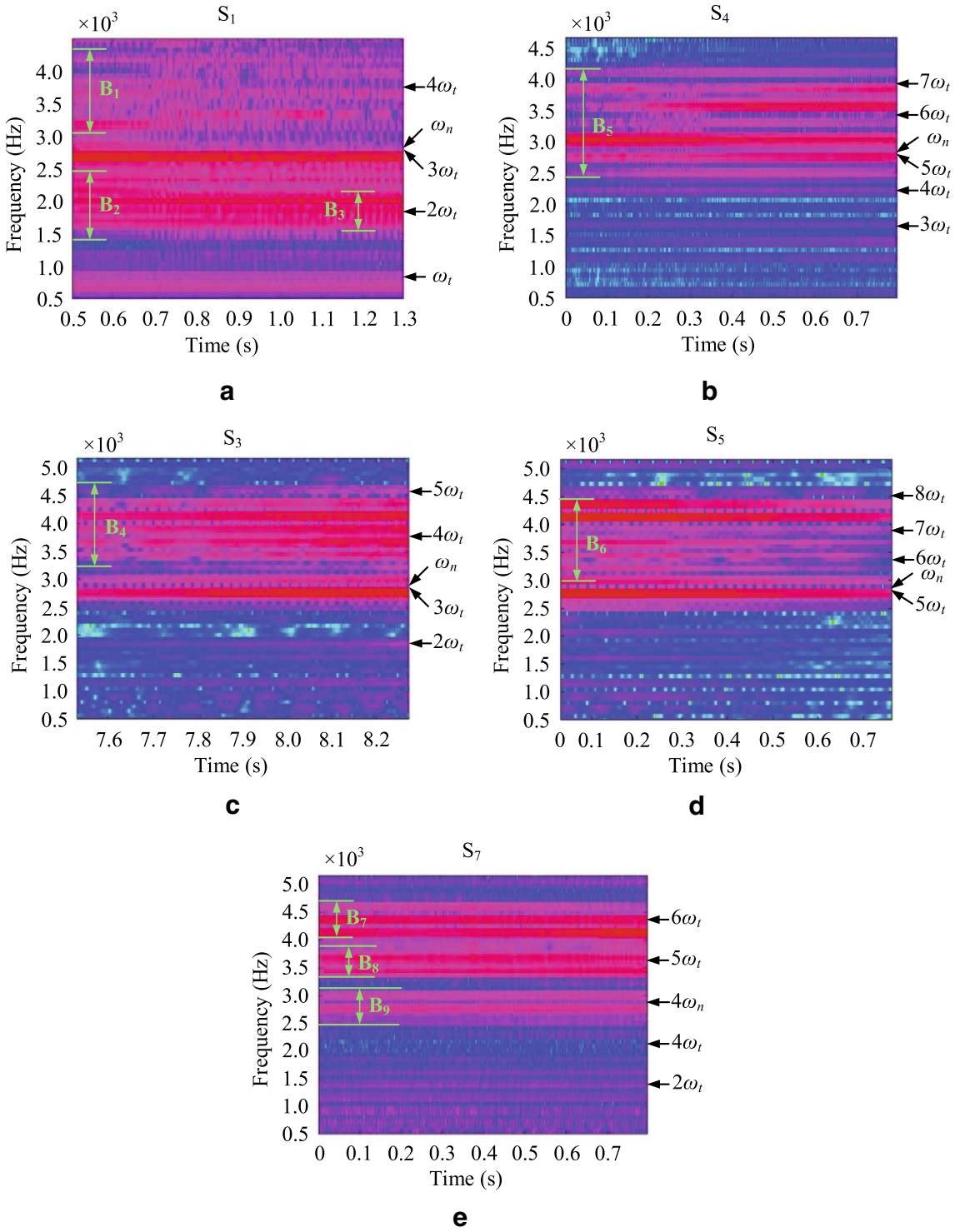

Fig. 8 STFT of acoustic signals about S1 and S4, S3 and S5, and S7. **a** S1 in chatter state. **b** S4 in chatter state. **c** S3 in transition state. **d** S5 in transition state. **e** S7 in stable state

of thin-walled parts is a time-varying system, but the sensitivity of STFT is too low to carry out multi-scale analysis of signals, and the influence of the time-varying and position-dependent characteristics of the thin-walled components milling on the chatter monitoring is neglected, which leads to numerical deviations in the processing results.

Further, through the STFT transformation of the above five acoustic signals, the following chatter monitoring results can be obtained. For S1 and S4, it can be seen from Fig. 8a, b that the dominant frequency band is distributed around the natural frequency, so it can be judged that S1 and S4 are in chatter state. For S3 and S5, it can be seen from Fig. 8c, d that the frequency band corresponding to the natural frequency is the brightest and plays a leading role, but the frequency band has no obvious change in color, and it is not easy to distinguish between S3 and S5 in chatter or transition state. For S7, it can be seen from Fig. 8e that the dominant frequency band is tooth pass frequency multiplication and it can be judged to be in stable state. However, there are too many redundant frequency bands in the time-frequency diagram, which directly interferes with chatter monitoring. Therefore, the chatter monitoring results obtained by STFT transform are inconsistent with those obtained by CMWT.

Secondly, at B1 (bandwidth 1) and B2 of the time-frequency diagram, the frequency band is significantly aliased, and the frequency band cannot be resolved. Among them, B3 is the most serious aliasing and it is impossible to identify typical frequency values. The phenomenon of aliasing is due to the low frequency resolution of STFT itself. Besides, the multi-modal and time-varying characteristics in the thin-walled part milling. Therefore, when the STFT is used for the time-frequency transformation of the acoustic signals of the thin-walled parts, aliasing occurs in the frequency domain, which becomes an intuitive obstacle to chatter monitoring and directly interferes with chatter monitoring.

Finally, in B4, B5, B6, B7, B8, and B9, there are many interference frequency bands except the tooth passing frequency multiplication, which is the effect of noise in the acoustic signal on the STFT.

In summary, although choosing a non-rectangular window—the Hamming window, which can avoid frequency leakage—STFT method still cannot evade the shortcoming that it is easy to be affected by noise. In the process of processing the sound signal of the thin-walled parts, due to the time-varying and position-dependent characteristics of the milling of thin-walled milling, STFT obviously shows low frequency resolution and poor sensitivity, which results in the frequency bands aliasing in the processing results, and seriously interferes with the chatter monitoring process. In addition, in the time-frequency diagram obtained by the STFT method, the numerical error of the frequency band is between ± 50 Hz, directly disturbing the chatter monitoring process, and it is easy to mislead the chatter monitoring of the milling of thin-walled parts. Because of the common effect of the above unfavorable factors, the STFT cannot adapt to the chatter monitoring of the thin-walled parts milling process. Meanwhile, the CMWT has shown obvious advantages in chatter monitoring of the thin-walled parts, which makes CMWT an effective method for chatter detection in thin-walled parts.

4.3 Verifications

In order to verify the correctness of CMWT chatter monitoring results, the SLD is predicted using the existing numerical method, and the machined surface topography of the workpiece is observed and checked.

4.3.1 Stability prediction results

Through the hammer mode experiment, the first-order natural frequency ω_n is 2713 Hz, which is very close to the first-order natural frequency (2873.1 Hz) in computer simulation. It can be obtained that the loss factor η of workpiece-fixture system is 0.06, from Eq. (8). Furthermore, from Eq. (11), the modal parameters corresponding to the discrete points, including the modal mass, modal stiffness, and modal damping of the first two orders can be obtained, as shown in Table 3.

When the modal parameters of the integer points on the path of the workpiece are obtained, the SLD can be drawn by the existing numerical methods, such as the time-space discretization method [37], which is much more efficient than the other method, and the SLDs are shown in Fig. 9. In Fig. 9, SLDs are given along x axis, which is the same direction with it in Fig. 1.

In SLDs, the green fill area indicates that chatter can occur at those cutting condition, the blue circle, the red pentagram, and the black triangle represent the cutting parameters in test

Table 3 The first two modal parameters corresponding to the discrete points

	First-order			Second-order		
Point position	Modal mass (kg)	Modal stiffness (×106 N/m)	Modal damp (N s/m)	Modal mass (kg)	Modal stiffness (×106 N/m)	Modal damp (N s/m)
0	0.0086	2.9355	8.1732	0.0038	3.2507	5.1170
1	0.0098	3.3323	7.8803	0.0069	5.8918	8.4753
2	0.0095	3.2400	7.5688	0.0156	13.2824	20.5343
3	0.0091	3.0895	7.3476	0.0626	50.7982	207.5289
4	0.0090	3.0782	7.2968	0.0633	51.0127	210.3251
5	0.0095	3.2736	7.4816	0.0152	13.0317	19.8927
6	0.0097	3.2964	7.8948	0.0064	5.5943	8.4011
7	0.0086	2.9602	8.2029	0.0039	3.2417	5.0988

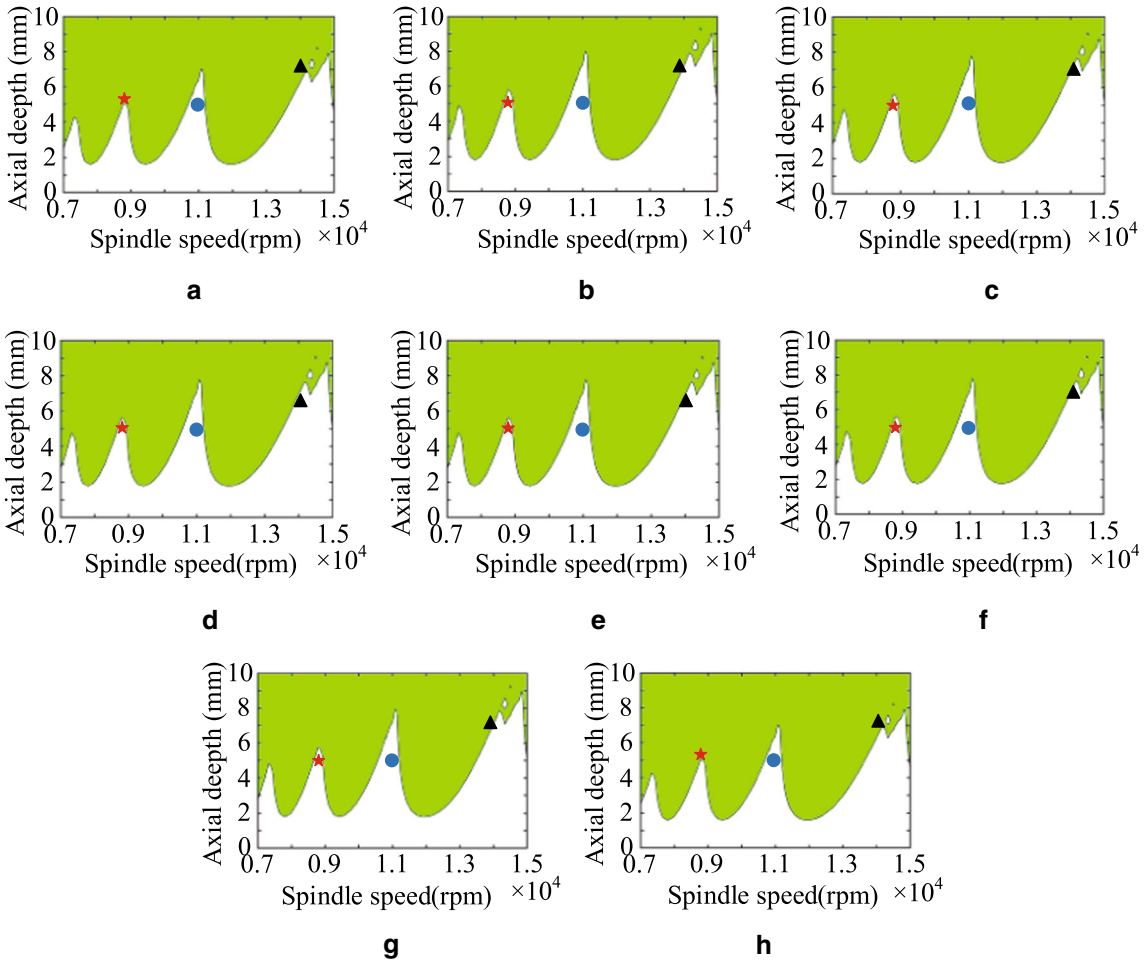

Fig. 9 Dynamic SLDs of different position points on workpiece. (Blue circle: $n = 11{,}000$ rpm, $ap = 5$ mm; red pentagram: $n = 8800$ rpm, $ap = 5$ mm; black triangle: $n = 14{,}000$ rpm, $ap = 7$ mm)

no. 5, test no. 8, and test no. 14, respectively. When the geometry is within the green fill area, the workpiece will chatter at this time. In contrast, when the geometry is outside the green fill area, the workpiece is in a stable state at this time. In test no. 5, chatter occurs at the positions of $x = 0$, 7 mm, as shown in Fig. 9a, h. In addition, the workpiece is in a stable state at the remaining integer points, as shown in Fig. 9b–g. In test no. 8, there is no chatter at all the integer points on the tool path, as shown in Fig. 9a–h. In test no. 14, the workpiece chatter at the position of $x = 0$, 1, 6, and 7 mm, as shown in Fig. 9a, b, g, h, and in a steady state at the rest of the integer points.

4.3.2 Morphology observation

In order to further verify the accuracy of the above judgment based on the CMWT results, the machined surface morphologies at different cutting positons are also observed by 3D confocal laser microscope and the surface roughness can be obtained at the same time, as shown in Fig. 10.

Figure 9 shows the surface morphology and cross-section curve of the machined surface. Through the diagram of cross-section curve, the surface roughness can be easily calculated. From Fig. 10, it can be observed that the machined surfaces corresponding to S_1 and S_3 have obviously vibration veins, and the cross-sectional curves and roughness values fluctuate greatly. Therefore, it can be confirmed that both S_1 and S_3 are in the chattering state which consistent with the judgment by CMWT. Correspondingly, the machined surface corresponding to S_2, S_6, and S_7 are smoother, and there is no significant fluctuation in the cross-section curves. Meanwhile, the value of the roughness is quite small. It can also be judged that S_2, S_6, and S_7 are in stable state. S_3 and S_5 can be intuitively found to be transition state by the trend of surface topography and cross-sectional curve. S_3 is the transition from chatter state to steady state, and S_5 is the transition from steady state to chatter state.

Through these observations, it is possible to verify the correctness of the chatter detection method (CMWT) for the thin-walled workpiece milling process. This means that the chatter signal can be monitored accurately and efficiently by using CMWT to process the acoustic signals in the milling process.

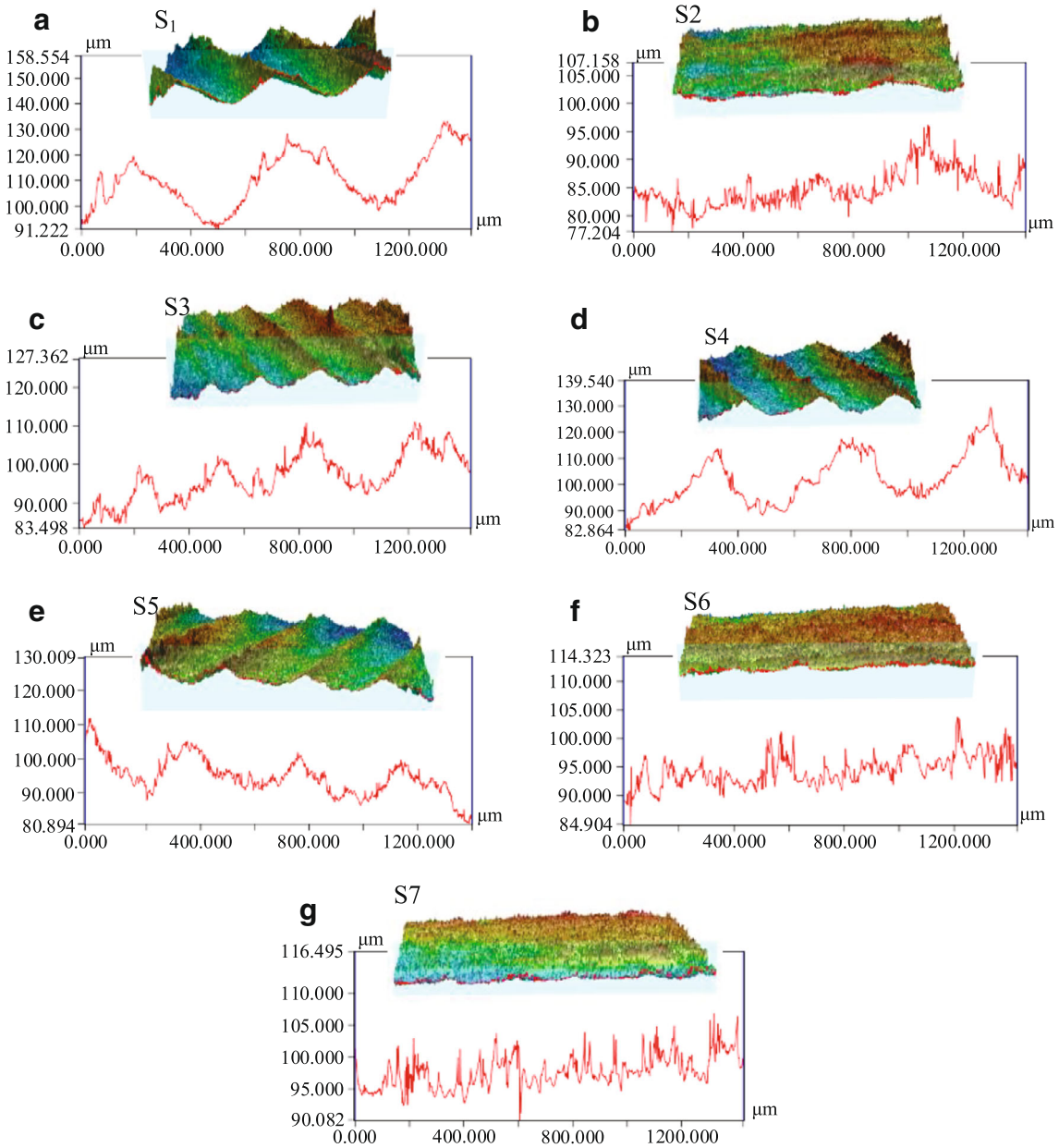

Fig. 10 The surface morphology and roughness of machined surface

5 Conclusions

In this paper, considering the time-varying and position-dependent characteristics of the thin-walled plate milling, and through the comparison with STFT method, CMWT is quite suitable for detecting milling chatter and obtaining the stability regions. In addition, the correctness of this method is verified by SLD and machined surface topography.

The advantage of this method is quite obvious. The Morlet wavelet (or cmor wavelet) has the optimal time-frequency resolution for milling process and has good locality in both time domain and frequency domain for milling acoustic signal. There is no redundant frequency band interference in the CMWT processing results, and the numerical error of the frequency band is so small that it can be ignored, and the process of the CMWT processing sound signal is not disturbed by noise. Through the analysis of the time-frequency diagram obtained by CMWT, the stability of thin-walled parts can be obtained intuitively. Meanwhile, CMWT improves the efficiency of chatter monitoring, effectively shortens the time of chatter monitoring, less than 0.2 s, and lays a solid foundation for the following online chatter detection. Especially, CMWT uses variable scale time-frequency factors to analysis of non-stationary acoustic signal, so as to realize multi-scale analysis and frequency analysis for different frequency bands of signals.

When using CMWT, once the natural frequency of the thin-walled workpiece and the tooth-through frequency of the milling system are obtained, it is possible to monitor whether or not chatter occurs by 2D and 3D time-frequency diagrams. When the parameters of the stability regions are obtained, the chatter in milling can be avoided, and the machining efficiency and machining accuracy can be remarkably improved.

Acknowledgments The authors are grateful to the financial supports of the National Natural Science Foundation of China (no. 51575319), Young Scholars Program of Shandong University (no. 2015WLJH31), the United Fund of Ministry of Education for Equipment Pre-research (no. 6141A02022116), and the Key Research and Development Plan of Shandong Province (no. 2018GGX103007).

Compliance with ethical standards

Conflict of interest The authors declare that they have no conflict of interest.

References

1. Song QH, Ai X, Tang WX (2011) Prediction of simultaneous dynamic stability limit of time-variable parameters system in thin-walled workpiece high-speed milling processes. Int J Adv Manuf Technol 55(9–12):883–889
2. Luo M, Luo H, Zhang D, Tang K (2018) Improving tool life in multi-axis milling of Ni-based superalloy with ball-end cutter based on the active cutting edge shift strategy. J Mater Process Tech 252: 105–115
3. Ryabov O, Mori K, Kasashima N (1998) Laser displacement meter application for milling diagnostics. Opt Lasers Eng 30(3–4):251–263
4. Devillez A, Dudzinski D (2007) Tool vibration detection with eddy current sensors in machining process and computation of stability lobes using fuzzy classifiers. Mech Syst Signal Process 21(1):441–456
5. Pérez-Canales D, Vela-Martínez L, Carlos Jáuregui-Correa J, Alvarez-Ramirez J (2012) Analysis of the entropy randomness index for machining chatter detection. Int J Mach Tools Manuf 62(1): 39–45
6. Lamraoui M, Thomas M, El Badaoui M (2014) Cyclostationarity approach for monitoring chatter and tool wear in high speed milling. Mech Syst Signal Process 44(1–2):177–198
7. Shao Y, Deng X, Yuan Y, Mechefske CK, Chen Z (2014) Characteristic recognition of chatter mark vibration in a rolling mill based on the non-dimensional parameters of the vibration signal. J Mech Sci Technol 28(6):2075–2080
8. Cao HR, Zhou K, Chen XF (2015) Chatter identification in end milling process based on EEMD and nonlinear dimensionless indicators. Int J Mach Tools Manuf 92:52–59
9. Gabriel RF, Alexandru E, Ionuț CC (2012) Method for early detection of the regenerative instability in turning. Int J Adv Manuf Technol 58(1–4):29–43
10. Huang P, Li J, Sun J, Zhou J (2013) Vibration analysis in milling titanium alloy based on signal processing of cutting force. Int J Adv Manuf Technol 64(5–8):613–621
11. Luo M, Luo H, Axinte D, Liu DS, Mei JW, Liao ZR (2018) A wireless instrumented milling cutter system with embedded PVDF sensors. Mech Syst Signal Process 110:556–568
12. Tangjitsitcharoen S, Saksri T, Ratanakuakangwan S (2015) Advance in chatter detection in ball end milling process by utilizing wavelet transform. J Intell Manuf 26(3):1–15
13. Liu Y, Wu B, Ma J, Zhang D (2016) Chatter identification of the milling process considering dynamics of the thin-walled workpiece. Int J Adv Manuf Technol 2016:1–9
14. Tsai NC, Chen DC, Lee RM (2010) Chatter prevention for milling process by acoustic signal feedback. Int J Adv Manuf Technol 47(9–12):1013–1021
15. Nair U, Krishna BM, Namboothiri VNN, Nampoori VPN (2010) Permutation entropy based real-time chatter detection using audio signal in turning process. Int J Adv Manuf Technol 46(1–4):61–68
16. Hynynen KM, Ratava J, Lindh T, Rikkonen M, Ryynänen V, Lohtander M, Varis J (2014) Chatter detection in turning processes using coherence of acceleration and audio signals. J Manuf Sci Eng 136(4):044503
17. Thaler T, Potočnik P, Bric I, Govekar E (2014) Chatter detection in band sawing based on discriminant analysis of sound features. Appl Acoust 77(77):114–121
18. Marinescu I, Axinte DA (2008) A critical analysis of effectiveness of acoustic emission signals to detect tool and workpiece malfunctions in milling operations. Int J Mach Tools Manuf 48(10):1148–1160
19. Delio T, Tlusty J, Smith S (2008) Use of audio signals for chatter detection and control. J Manuf Sci Eng 114(2):146
20. Li X, Guan XP (2004) Time-frequency-analysis-based minor cutting edge fracture detection during end milling. Mech Syst Signal Process 18(6):1485–1496
21. Liu HQ, Chen QH, Li B, Mao XY, Mao KM, Peng FY (2011) On-line chatter detection using servo motor current signal in turning. Sci China Technol Sci 54(12):3119–3129
22. Kuljanic E, Sortino M, Totis G (2008) Multisensor approaches for chatter detection in milling. J Sound Vib 312(4–5):672–693
23. Tangjitsitcharoen S, Pongsathornwiwat N (2013) Development of chatter detection in milling processes. Int J Adv Manuf Technol 65(5–8):919–927
24. Song QH, Liu ZQ, Wan Y, Ju GG, Shi JH (2015) Application of Sherman-Morrison-Woodbury formulas in instantaneous dynamic of peripheral milling for thin-walled component. Int J Mech Sci 96-97:79–90
25. Liu C, Zhu L, Ni C (2017) The chatter identification in end milling based on combining EMD and WPD. Int J Adv Manuf Technol 91(9–12):1–10
26. Sheng Q, Zhao J, Wang T (2016) Three-dimensional stability prediction and chatter analysis in milling of thin-walled plate. Int J Adv Manuf Technol 86(5–8):2291–2300
27. Fang N, Pai PS, Edwards N (2014) A method of using Hoelder exponents to monitor tool-edge wear in high-speed finish machining. Int J Adv Manuf Technol 72(9–12):1593–1601
28. Mallat SG (2009) A wavelet tour of signal processing: the sparse. way 31(3):83–85
29. Yao Z, Mei D, Chen Z (2010) On-line chatter detection and identification based on wavelet and support vector machine. J Mater Process Technol 210(5):713–719
30. Cao HR, Lei YG, He ZG (2013) Chatter identification in end milling process using wavelet packets and Hilbert-Huang transform. Int J Mach Tools Manuf 69(3):11–19
31. Jiang AY, Zhang C (2006) Hybrid HMM/SVM method for predicting cutting chatter. Proc SPIE Int Soc Opt Eng 62801:8

32. Chen GS, Zheng QZ (2017) Online chatter detection of the end milling based on wavelet packet transform and support vector machine recursive feature elimination. Int J Adv Manuf Technol 5:1–10
33. Zhang Z, Li H, Meng G, Tu X, Cheng C (2016) Chatter detection in milling process based on the energy entropy of VMD and WPD. Int J Mach Tools Manuf 108:106–112
34. Sun Y, Zhuang C, Xiong Z (2014) Real-time chatter detection using the weighted wavelet packet entropy. Int Conf Adv Intel Mech 2014:1652–1657
35. Wang L, Liang M (2009) Chatter detection based on probability distribution of wavelet modulus maxima. Robot Comput Integr Manuf 25(6):989–998
36. Shi JH, Song QH, Liu ZQ, Ai X (2017) A novel stability prediction approach for thin-walled component milling considering material removing process. Chin J Aeronaut 30(5):1789–1798
37. Song QH, Shi JH, Liu ZQ, Wan Y (2016) A time-space discretization method in milling stability prediction of thin-walled component. Int J Adv Manuf Technol 2016:1–15
38. Cao H, Yue Y, Chen X, Zhang X (2016) Chatter detection in milling process based on synchrosqueezing transform of sound signals. Int J Adv Manuf Technol 2016:1–9
39. Lin J, Qu LS (2000) Feature extraction based on Morlet wavelet and its application for mechanical fault diagnosis. J Sound Vib 234(1): 135–148
40. Yi H, Shu H (2012) The improvement of the Morlet wavelet for multi-period analysis of climate data. Compt Rendus Géosci 344(10):483–497
41. Ao Y, Qiao G (2010) Prognostics for drilling process with wavelet packet decomposition. Int J Adv Manuf Technol 50(1–4):47–52
42. Prakash M, Kanthababu M, Rajurkar KP (2015) Investigations on the effects of tool wear on chip formation mechanism and chip morphology using acoustic emission signal in the microendmilling of aluminum alloy. Int J Adv Manuf Technol 77(5–8):1499–1511
43. Seemuang N, Mcleay T, Slatter T (2016) Using spindle noise to monitor tool wear in a turning process. Int J Adv Manuf Technol 86(9–12):2781–2790